Systems Therapeutics for Axonal Regeneration in the Central Nervous System

Mustafa M. Siddiq[1], Yana Zorina[1], Jens Hansen[1], Arjun S. Yadaw[1], Vera Rabinovich[1], Sarah M. Gregorich[2], Yuguang Xiong[1], Ehud Kaplan[1,3], Robert D. Blitzer[1], Marie T. Filbin[4]*, Christopher L. Passaglia[2] and Ravi Iyengar[1]

[1]Department of Pharmacological Sciences and Systems Biology Center New York , Icahn School of Medicine at Mount Sinai , New York , NY, 10029
[2]Departments of Chemical & Biomedical Engineering, 4202 E. Fowler Ave, Tampa, FL, 33620
[3]Current Address: NUDZ (National Institute of Mental Health, Klecany, & Charles University, Prague, Czechia)
[4]Department of Biological Sciences, Hunter College, City University of New York NY, 10065
*Deceased January 15, 2014

Address correspondence to
Ravi Iyengar
Dept of Pharmacological Sciences, Box 1215
1425 Madison Rm 12-70
New York NY 10029
Ravi.iyengar@mssm.edu

THIS IS A WORKING PAPER SUBJECT TO FURTHER REVISIONS

Supported by NIH grants R01GM54508 and Systems Biology Center grant P50GM071558

Abstract

Injured central nervous system (CNS) axons do not regenerate, due to lack of intrinsic capacity of the neurons and the inhibitory environment at the injury site. Currently, there are no drugs or drug combinations to promote axonal regeneration in the injured spinal cord or optic nerve. We used a systems pharmacology approach to develop a four-drug combination with the potential to increase neuronal capacity by regulating multiple subcellular processes at the cell body to trigger long neurites in inhibitory environments. Dynamical computational models of neurite outgrowth showed that the transcriptional effects of drugs applied at the cell body when combined with drugs that work locally near the site of the injured axons could produce extensive synergistic growth. We used the optic nerve crush in rats to test the drug combinations. We intravitreally injected two drugs, HU-210 (cannabinoid receptor-1 agonist) and IL-6 (interleukin 6 receptor agonist) to stimulate retinal ganglion cells (RGCs) whose axons had been crushed, and applied two drugs in gel foam, taxol to stabilize microtubules and activated protein C (APC) to potentially clear the injury site debris field. Morphology experiments using the injured optic nerve show that the four-drug combination promotes robust axonal regeneration from the RGC to the chiasm. Electrophysiologically the four-drug treatment restored pattern electroretinograms (pERG), and about 25% of the animals had detectable visual evoked potentials (VEP) in the brain. We conclude that systems pharmacology-based drug treatment can promote functional axonal regeneration after nerve injury.

Introduction

Injury in the adult CNS is often permanent due to lack of ability of severed axons to regenerate. The inability to regenerate axons is attributed to two major causes: lack of intrinsic capacity of the CNS neurons in adult mammals to regenerate, and the presence of extracellular factors that inhibit axonal outgrowth (1-4). Myelin-associated molecules are thought to play a major role in inhibiting axonal regeneration (2,5). In addition to the extrinsic inhibition, lack of appropriate activation of intracellular signaling pathways is also thought to play a role. Prominent among these are the MTOR (6) and STAT3 (7-8) pathways. Simultaneous inactivation of PTEN, an endogenous inhibitor of the MTOR pathway, and SOCS 3, an endogenous inhibitor of the STAT3 pathway, led to robust and sustained axonal regeneration (9). Recently it has been shown that sustained activation of the MTOR pathway by genetic manipulation when combined with visual stimulation leads to extended regeneration of optic nerve axons such that they reach the brain (10). Transcriptomic analyses of DRG neurons following peripheral nerve injury have identified the potential involvement of numerous signaling pathways including neurotrophins, TGFβ cytokine, and JAK-STAT pathways (11). Using these transcriptomic data and the Connectivity MAP, these researchers identified a drug ambroxol, a Na^+ channel inhibitor that promoted axon regeneration after optic nerve crush in mice (11). Taken together, these observations suggest that drug therapy based on regulation of subcellular processes including cell signaling pathways could be a feasible approach to promote axon regeneration of nerve injury.

We have been studying signaling through the Go/i pathway for over two decades and found that activated Gαo activates STAT3 to promote oncogenic transformation (12). Studies on cannabinoid receptor-1 (CB1R)-stimulated Neuro-2A cells indicated that this receptor, acting through the GTPases Rap, Ral and Rac, activates Src which in turn activates STAT3 to control neurite outgrowth (13-14). A more extensive study identified a complex upstream signaling network that controls STAT3 and CREB to regulate neurite outgrowth (15). These studies indicated that multiple receptors could regulate STAT3 to drive neurite outgrowth. IL-6 had been shown to promote neurite outgrowth in a PC-12 variant, and to overcome myelin-mediated inhibitors to promote neurite outgrowth in primary neurons (7, 16). We showed that submaximal, potentially therapeutic concentrations of the CB1R agonist HU-210 together with IL-6 could activate STAT3 in a sustained manner and induce neurite outgrowth in both Neuro2A cells and rat cortical primary neurons (17). Based on these observations we decided to test if a combination of these two drugs could promote axonal regeneration *in vivo* in the CNS using the rat optic nerve crush model.

In designing these studies, we anticipated that stimulating signaling only in the injured neurons probably would not lead to long distance axon regeneration to the brain, and that we would need to modulate additional loci for extended axonal growth. Hence we sought to develop a systems level reasoning-based combination therapy.

We sought to identify drugs that would modulate subcellular function in a spatially specified manner in the cell body and axon. We could then utilize this regional information to develop a drug combination with the potential for treating CNS nerve injury by promoting long-range axonal regeneration. Since transcriptional regulation is critical for neurite outgrowth, we reasoned that CB1R and IL6R actions are likely to be in the cell body. We looked for subcellular processes in the axon that could be potential drug targets. We utilized computational dynamical models of neurite outgrowth (18) to predict how different spatially specified processes could promote axonal regeneration. Based on these simulations we focused on microtubule growth, which is required for axon regeneration. Microtubules are stabilized by taxol, which has been shown to promote axonal regeneration (19). As axonal regeneration is inhibited by uncleared cell remnants at the site of injury, we hypothesized that such inhibition could be due the incorporation of membrane vesicles at the growth cone. Treating the site of injury to potentially clear the site of inhibitory agents and reduce inflammatory response could also contribute to axonal regeneration. Based on these considerations we chose a protease that could act locally to reduce the debris field and inhibit inflammation. We selected APC, which is a serine protease endogenous to the coagulation system (20) that is thought to be anti-inflammatory, and which promotes neuronal repair by stem cells in mice (21). In another study we have independently observed that APC can promote limited axonal regeneration of crushed optic nerve in rat (22). Hence we decided to test if a combination of these four drugs, two applied at the cell body and two at the axon at the site of injury, promoted long distance regeneration such that visual stimulation led to restoration of physiological function.

Results

Neurite outgrowths in microfluidic chambers with IL-6 and HU-210:

We had found that submaximal concentrations of IL-6 and HU-210 in combination could have a synergistic effect on neurite outgrowth for rat cortical neurons in primary culture (17). We tested if this synergistic effect could be observed for regeneration of growing neurites that had been severed *in vitro*. For these experiments we used microfluidic chambers, where the cell bodies could be compartmentalized from the growing neurites (Figure 1-I). We plated primary rat cortical neurons on a permissive substrate in these chambers, and allowed them to grow long neurites. To mimic axotomy, we lesioned all the neurites in the chambers on the right side (see Figure 1-I&IIA) and then added HU-210 and IL-6. After axotomy, IL-6 and HU-210 combination had a more robust effect in promoting neurites to grow when applied directly to the neuronal cell body (soma). Though some growth was observed when added to the axonal compartment, it was significantly less than when added to the soma. We then repeated the experiment using myelin, a non-permissive substrate (Figure 1-II). We observed that addition of IL-6 and HU-210 to the cell bodies promoted longer growth of axotomized processes in the presence of myelin, compared to either treatment alone. When using whole myelin as substrate in a neurite outgrowth assay, we found IL-6 and HU-210 still promoted neurite outgrowth of cortical neurons and overcame the inhibitory effects of myelin (Figures 1-III & IV). We found in cortical neurons, as previously reported in Neuro2A cells (17), that the combination of IL-6 and HU-210 treatment stimulated STAT3 by phosphorylation at Tyr705 (see Fig 1-V),which we normalized to total STAT3 levels and βIII-tubulin levels.

A four-drug combination promotes optic nerve regeneration to the chiasm

We used Fischer (albino) rats for the first set of in vivo studies on nerve regeneration. The right optic nerve was crushed as described (23). After injury we treated the injured eye with HU-210 and IL-6 injected intravitreally. After two weeks, we evaluated for regeneration. We detected regenerated axons by the traditional method of sectioning the nerve and immunostaining for GAP-43 (see Fig2A & B). The majority of the crushed axons without treatment had no detectable GAP-43-labeling even 0.2 mm away from the crush site, however intravitreal injection of a combination of IL-6 & HU-210 resulted in detectable axons nearly 3 mm away from the crush site, as demarcated by the white arrows (Figure 2B) . To verify this finding and to assess regeneration within the entire nerve and not just one thin section, we labeled the regenerating axons with cholera toxin-B subunit (CTB) (24) and chemically cleared the nerves using the 3-DISCO technique (25), and obtained maximum intensity projection images using an Olympus Multiphoton microscope (see Fig2C & D). Using the 3-DISCO technique, we could image the crush site from proximal to distal end, and could look at the Z-stack to determine if the crush was complete with no fibers that appeared to be “spared”. In Supplementary Figure 2C, we provide an image of a CTB-labeled uninjured nerve, where we see the extent of long intact

axons. In Supplementary Figure 2D, we provide an image of a nerve with an incomplete crush, as we can see the top edge has crushed fibers while the bottom edge has long uninjured fibers; such samples were subsequently removed from our study. When animals received intravitreal injections of IL-6 & HU-210, we could observe CTB-labeled fibers 2-3 mm from the crush site, with several long axons detected as shown in the magnified region over Fig 2D. At this stage we wanted to determine how the drug treatment affected the electrophysiological responses by recording pattern ERGs. We discontinued using the Fischer rats, as their Albino phenotype made them unsuitable for retinal electrophysiology.

We continued the study with pigmented Long-Evans rats. We first reproduced our observations from the Fischer rats (Fig. 3). After the optic nerve was crushed, regeneration was not observed in animals that received either no drug treatment or treatment with submaximal concentrations of IL-6 or HU-210 individually, as assessed by CTB-labeled fibers 0.2 mm away from the crush site (see Figs. 3A-C). The combination of intravitreal IL-6 and HU-210 resulted in significant axon growth beyond the crush site (over 0.5 mm) (Fig. 3D), but using the same drug concentrations as in the Fischer rats yielded a less robust response in the Long-Evans rats.

Our overall goal here was to devise a drug therapy that would provide sufficient regeneration after the optic nerve crush so that we could restore communication between the eye and the brain. The observations here and our previous biochemical data (15, 17) indicate that the effects of HU-210 and IL-6 are likely to be through biosynthetic processes. Since this treatment did result in sufficiently long regeneration such that the regenerated nerve crossed the chiasm to the brain, we looked for additional subcellular processes that could be targeted by drugs. For this we utilized a dynamical model of neurite outgrowth that we have recently developed (18) that is focused on understanding how activities of groups of subcellular processes are balanced to produce a whole cell response. In this computational model we studied how microtubule growth and membrane vesicle transport and fusion at the growth cones are together responsible for neurite and axon regeneration. These simulations indicated that simultaneously regulating the microtubule dynamics and membrane vesicle dynamics could greatly enhance axon regeneration. Taxol is known to stabilize dynamic microtubules and thus promote microtubule elongation and axonal regeneration (19). To regulate membrane vesicle delivery-related subcellular processes, we focused on external inhibitors of axonal growth, including myelin-associated proteins such as Nogo. Biochemical experiments have shown that Nogo receptors and gangliosides mediate glycoprotein inhibition of neurite outgrowth (26) and binding of extracellular agents such as Nogo to gangliosides can promote endocytosis (27), thus disrupting membrane delivery to the growth cone. Since the site of injury contains many such myelin-related proteins, to relieve inhibition we decided to test the application of a protease that could act locally. For this we chose APC (activated protein C), which has been reported to promote neuronal repair (21). We used gel foam to apply taxol to the site of injury, and APC singly or in combination with HU-210 and IL-6 applied at the cell body through intravitreal injection. These results are shown in Figure 4.

Taxol alone in gelfoam had a modest effect on promoting some regenerating fibers as reported earlier (Fig. 4A) (28). Combining IL-6 and HU-210 with taxol gelfoam did give a more robust response compared to the 3 agents individually or IL-6 and HU-210 combined, growing over 0.5 mm away from the crush site (Fig. 4B). APC alone promoted significant axonal regeneration about 1 mm past the crush site (Fig. 4C). However, none of the 4 drugs tested could promote extensive axonal regeneration individually. We then tested a four-drug combination with intravitreal injection of HU-210 and IL-6 to deliver these agents to the retinal ganglion cell body and application of taxol and APC in gelfoam at the site of injury. We sacrificed the animal after 3 weeks of drug treatment. Three days prior to euthansia we intravitreally injected CTB coupled to Alexa-488 to visualize the regenerated axons. The whole nerves were chemically cleared using the 3DISCO technique (25). We observed that 5 out 19 animals tested had regenerating axons that could detected at the chiasm, a distance of 7.5 mm from the crush site (Fig. 5). Another three out of 19 animals with the four-drug treatment combination had more modest axonal regeneration about 3 mm from the crush site (see Table 1).

A number of control experiments are shown in the Supplementary Figures. In Supplementary Figure 2 (SFig. 2), we include magnified images of sections demarcated by the asterisk in Figure 5. In SFig. 2A we have the image just to the left of the asterisk and in SFig. 2B the image is taken from just below the asterisk, where punctated CTB labeling is observed throughout the nerve. In SFig. 2C, we have an uninjured nerve with CTB labeling, showing the full extent of fibers with the optic nerve bundle. In SFig. 2D, we show an example of an incomplete crush. With the 3-DISCO technology we can examine all the CTB-labeled axons in the nerve bundle, here we can see spared fibers toward the bottom edge demarcated by an arrow. When we observed such a sample, the animal was disqualified from the study. Alternatively, some nerves are not labeled with CTB but using the iDISCO technique we labeled the whole nerve with antibodies against GAP-43 and then chemically cleared them (see Supplementary Figure 3 (SFig. 3)) (29). Both CTB-labeled and GAP43-immunostained whole nerves are imaged using a multiphoton microscope. In SFig. 3, we see the crush site where GAP-43 axons are regenerating past the crush site (left panel), and in the right panel we have GAP-43-labeled axons detected in the chiasm, as demarcated by the arrows. All of these control experiments provide additional support that the CTB labeled nerves observed in Figure 5 are regenerated axons.

The four-drug combination treatment partially restores electroretinograms and visual evoked potential in the brain of animals subjected to the optic nerve crush

We next tested if the morphologically observable regeneration led to restoration of electrophysiological functional responses. To determine if the four-drug combination could improve overall retinal electrophysiology, we recorded pattern electroretinograms (pERG), where a pattern stimulus (contrast reversing checkerboards) is associated with detecting activity specifically in the retinal ganglion cells (Fig. 6A) (31). In normal non-injured eyes, pERG is

detected by a small initial negative component approximately 35 ms (N35) after pattern reversal, followed by a larger positive component between 45-60 ms (P50), and finally a large negative component at 90-100 ms (N95) (32). In Figure 6A, we show that both non-injured eyes of two animals have the characteristic N35, P50, and N95 signals. The injured eye of the control animal with only vehicle injections had an aberrant pERG compared to its non-injured eye (Figure 6, left panel). However, injured animals that received the four-drug combination treatment (right panel) showed improved pERG in the injured eye compared to vehicle controls, and approaching pre-injury responses similar to its non-injured eye. The representative recordings are raw data that are not normalized, where we show recordings of the non-injured eye (in blue) as an internal control, compared to the injured eye in red. However, pERG are indicative of the retinal neuronal cell bodies and not of the axons themselves. In order to have a better understanding of function beyond the site of damage, we stimulated the retina with a graded series of light (0.001 to 100% intensity) and recorded flash ERGs (fERG) (see Supplementary Figures 4A), while simultaneously recording corresponding signals in the brain as visual evoked potentials (VEP). A full graded series response to light flash is shown in SFig. 4. Representative fERG traces are shown in SFig. 4A. Panel I displays the response in an uninjured nerve. Panel II is the response in the injured vehicle-treated condition, where we see a strong reduction in the fERG signals at all intensities, consistent with neurodegeneration that occurs due to the crush. Panel III shows the response in the injured drug-treated condition, where fERG are approaching baseline levels, suggesting that the therapy is neuroprotective as well as promoting axonal regeneration. In Fig. 6B, we show the VEP for the uninjured eye, where we observe two different waveforms. At lower intensities, 0.001 and 0.01%, we see a slow monotonic response to light, but at higher intensities (0.1% and above, see SFig. 4B) we observe a faster and more compound action potential response (Fig. 6B). This VEP observed in an uninjured eye is lost in the injured eye of an animal with vehicle-only treatment, where at higher intensities of light above 10%, we observe only noise (see Fig. 6C). In contrast, 4 out of 13 injured animals treated with the four-drug combination showed VEP signals. At higher light intensities (50 and 100% in Fig. 6D), there is a slow and monotonic response to light, similar to what we observed in the uninjured eye at lower light intensities (see 0.01% in Fig. 6B) indicating that the four-drug treatment is restoring some function to the injured nerve. Data of complete VEP recordings for three individual animals for the uninjured eye, injured with vehicle-only, and injured with four-drug treatment are shown in Supplementary Figures 4A-D. We performed statistics on the animals with restored VEP activity using Z-score analysis, using a Z-score of 3 above RMS noise as a criterion for VEP detection, and found that responses were statistically more likely than in injured vehicle-treated animals

Discussion

Pathophysiology arising from injury or severing of nerves results in paralysis and is most often permanent. Currently there are no therapies to restore function; although regeneration through stem cell based therapies have been proposed (30). There are no reports of drug therapy that can restore function after nerve injury. This is thought to be due to both lack of intrinsic capacity of adult neurons to regenerate functional axons, and the inhibitory factors that prevent regrowth of axons beyond the injury site. This is the first proof-of-principle study that shows that drug therapy can be used to treat nerve injury.

We designed drug therapy for this complex pathophysiology by considering the multiple subcellular processes involved in axonal regeneration. We focused on drugs that would increase neuronal capacity for regeneration and enhance the ability of the axons to grow longer by modulating local subcellular processes in the axonal shaft. Here we made the assumption that the process of neurite outgrowth in vitro involves many if not all of the subcellular processes that neurons use regenerate axons in vivo. Cell signaling experiments in our laboratory over a long period had shown that transcriptional regulation through STAT3 and CREB played a major role in neurite outgrowth (12, 17). Independent studies had shown a role for the cAMP pathway (2) and SOCS3, a STAT inhibitor (9). Hence we reasoned that application of receptor ligands that stimulate the STAT3 pathway among other transcriptional regulators (15) could increase the intrinsic capacity of neurons to regenerate. Since the CB-1 receptors and IL-6 receptors are expressed in adult neurons, we selected agonists for these receptors as regenerative drugs. In vitro experiments showed that application of these drugs at the cell body was more effective in promoting regeneration, and hence in vivo we applied the drug at the cell body as well. As we used the optic nerve crush experimental model, we injected the receptor agonists intravitreally so that they could act RGCs. This resulted in modest but significant drug-stimulated axon regeneration beyond the site of injury. These experiments provided us with an important guideline: that not only should we select the right subcellular process to target, but also that the drug should be applied as the right location. Using this reasoning we selected the two core sets of subcellular processes that function within the growing axon: microtubule growth and membrane expansion at the growth cone as subcellular processes that could targeted by drugs. Since taxol stabilizes dynamic microtubules to convert them to stable microtubules, thus allowing axonal processes to grow, we applied taxol to the growing axonal regions. Integrating observations in the literature (26, 27) we reasoned that the debris at the injury site including myelin associated proteins might inhibit axonal growth by modulating membrane endocytosis and thus blocking exocytotic delivery of membranes to the growth cone. Hence we selected a locally active protease that could clear the debris field and block these inhibitory agents. Our experiments show that this combination of increasing capacity at the cell body and modulating subcellular processes in the growing axon allowed us to obtain substantial regeneration, such that we were able to partially restore electrophysiological communication from the eye to the visual cortex. Thus, the systems therapeutic approach provides a rational basis for design of therapies for complex pathophysiologies such as nerve regeneration in the CNS.

Although it is encouraging that we have an identifiable path for the design of rational therapeutics, much further work is needed to translate these findings into viable treatments even in animal models. We have not considered dosing regimens or adverse events associated with this drug therapy. We also need to establish the relationship between the extent of recovery of electrophysiological function and vision-dependent whole animal behavior. These types of experiments will form the basis for future studies. Nevertheless, since observations in the optic nerve crush model are most often applied to spinal cord injury, it will be useful to test if this four-drug combination can reverse spinal cord injury and restore movement.

Methods

Rat primary cortical neuron cultures – Rat primary cortical cultures were dissected from postnatal day 1 Sprague Dawley rat brains. Cortices were incubated twice for 30 min with 0.5 mg/ml papain in plain Neurobasal (NB) media (Invitrogen) with DNase. Papain activity was inhibited by brief incubation in soybean trypsin inhibitor (Sigma). Cell suspensions were layered on an Optiprep density gradient (Sigma) and centrifuged at 1900 x *g* for 15 min at room temperature. The purified neurons were then collected at 1000 x g for 5 min and counted.

Neurite outgrowth assay - Suspensions of purified CNS myelin (1–2 µg/well) were plated in chamber slides and desiccated overnight to create a substrate of myelin on eight well chamber slides as previously described (34). Primary cortical neurons were diluted to 35,000 cells/ml in NB supplemented with B27, L-glutamine and antibiotics, and we seeded 300 µl of the cell suspension to each well and incubated for 24 h. To quantify the outgrowth we immunostained using a monoclonal anti-βIII tubulin antibody (Tuj1;Covance) and Alexa Fluor 568-conjugated anti-mouse IgG (Invitrogen). For quantification, images were taken, and the length of the longest neurite for each neuron was measured using MetaMorph software (Molecular Devices).

For western blots primary neurons were treated with IL-6, HU-210 or both and lysed in radioimmunoprecipitation assay (RIPA) buffer (50 mM Tris-HCl, pH 7.5; 100 mM NaCl; 1% Nonidet P-40; 0.5% deoxycholic acid; 0.1% SDS; 1 mM EDTA) supplemented with protease and phosphatase inhibitors. After determination of protein concentration, the cell lysates were subjected to immunoblot analysis using standard procedures and visualized by enhanced chemiluminescence (ECL). Polyclonal rabbit antibodies directed against phospho-STAT3 and total STAT3 were from Cell Signaling Technology Inc.

Rat optic nerve regeneration in vivo:

Optic nerve crush experiments. Adult male Sprague-Dawley or Long Evans rats (250–280 g, approximately 8-10 weeks old) were anesthetized with isoflurane and placed in a stereotaxic frame. The right optic nerve was exposed and crushed with fine forceps for 10 s. For our four-drug treatment (all drugs were from Sigma except where noted), animals received a single 2.5 µl of intravitreal (intraocular) injection of either 1% DMSO (n=9) or combination of IL-6 [5

µg/ml] and HU-210 [300 µM] (n=19) immediately after the crush and gelfoam, soaked in APC [4.1 mg/ml] (Haematologic Technologies, Inc) and taxol [5 µM], was placed over the injury site. 3 days later, we confirmed that lens injury was avoided and injected for a second time intravitreally with 2.5µl of IL-6 [5 µg/ml] and HU-210 [300 µM]. We also ran individual controls for all drugs tested (n=5 for each). 3 days prior to sacrificing we labelled the regenerating axons with 5 µl of 1 mg/ml cholera toxin B (CTB) coupled to Alexa-488, which we intravitreally injected. Animals were anesthetized with ketamine (100 mg/kg) and xylazine (20 mg/kg) injected intraperitoneally, and the brain was fixed by transcardial perfusion with cold 4% PFA in PBS (pH 7.4) after a 21-day postsurgical survival period. The optic nerves and chiasm attached were dissected out and post-fixed in 4% PFA overnight at 4^{o}C, rinsed for one hour in PBS, and then prepared for chemical clearing. Since the advent of the 3DISCO clearing techniques, we are no longer dependent on sectioning the tissue; this method also eliminates bias associated with artifacts produced by sectioning. The whole nerve was exposed to a graded series of dehydrations with tetrahydrofuran (THF; Sigma) diluted in water: 50%, 70%, 80%, 100% and 100% again. Each THF dilution was for 20 min at room temperature on an orbital shaker (25). This was followed by dicholoromethane (Sigma) for 5 min at room temperature on an orbital shaker, and then by the clearing agent, dibenzyl ether (DBE; Sigma) overnight at room temperature on an orbital shaker. Microscope slides were mounted with Fastwell chambers (Electron Microscopy Sciences) and the cleared sample was placed on the slide and covered with DBE and a No. 1.5 micro coverglass. We imaged the whole sample on an Olympus Multiphoton microscope with a 25X water immersion lens. All procedures were approved by the IACUC of the Icahn School of Medicine at Mount Sinai in accordance with NIH guidelines.

Electrophysiological recordings: All electrophysiology was performed using Long Evans (pigmented) rats. Pattern electroretinograms (pERG) were performed at the Icahn School of Medicine at Mount Sinai (Iyengar lab). Rats were anesthetized with ketamine and xylazine 21 days post-surgery and positioned in a device designed for measuring pERGs (LKC Technologies, UTAS-2000). Contact lenses embedded with gold electrodes were placed on the corneas, and light-adapted responses of both eyes were recorded to a contrast-reversing checkerboard pattern displayed on a monitor located 11 cm in front of the corneas (32). Responses to 300 pattern reversals (spatial frequency: 0.033 cycle/degree; contrast: 100%, temporal frequency: 2 Hz) were averaged to estimate the pERG.

Flash ERGs (fERG) and visual evoked potentials (VEP) were performed at USF Tampa (Passaglia lab) (33). Rats were anesthetized with ketamine and xylazine and placed on a heating pad. Cannulas were surgically inserted into the femoral vein for intravenous drug delivery and the trachea for mechanical ventilation if necessary. Anesthesia was maintained with intravenous infusion (all dosages are mg/kg/hr) of ketamine (30), xylazine (1.5), dextrose (600), and physiological saline. The animal was mounted in a stereotactic apparatus in a light-tight booth. Heart rate was monitored with ECG electrodes, and body temperature was monitored with a

rectal thermometer. The eyes were covered with clear contact lenses, and pupils were dilated with a mydriatic. Flash stimuli were produced by a green LED encased in an opaque tube (1.7 cm diameter) that blocked the escape of light. The tube exit was fitted with a hemispherical diffuser that covered the eye to provide Ganzfeld illumination. fERGs were recorded with a ring-shaped gold electrode placed on the cornea. Platinum needle electrodes were inserted in the temples and tail to serve as references and ground, respectively. VEPs were recorded from both cortical hemispheres via two 1.3 mm steel screws inserted through the skull 7 mm posterior to Bregma and ±2.5 mm lateral to the midline. Recorded signals were differentially amplified (10,000X) and filtered (0.1-1,000 Hz) by a multichannel bioamplifier and digitized at 1 kHz. Animals were dark adapted for 15 min prior to data collection, and then baseline fERG and bilateral VEP data were collected simultaneously for a series of 100 brief (10 ms) flashes with an interstimulus interval of 3 s to allow for recovery of visual sensitivity. Average responses were measured for flash series of increasing intensity in 7 logarithmic steps to a maximum of 1.32 log cd·s/m^2 (100% condition) presented to one eye and then the other. Since approximately 90% of the fibers in the rat optic nerve cross to the opposite side to innervate the brain, when we flashed light and recorded from the right injured optic nerve we recorded the corresponding VEP on the left side of the brain. All procedures were approved by the IACUC of the USF at Tampa in accordance with NIH guideline.

Statistical analyses. Except where noted, analyses were performed using GraphPad Prism software, and data are represented as mean ± SEM. Statistical significance was assessed using paired one-tailed Student's *t* tests to compare two groups, and one-way ANOVAs with Bonferroni's *post hoc* tests to compare between three or more groups.

To evaluate the effectiveness of four-drug treatment in restoring the VEP following injury, we analyzed traces from each animal to detect physiological responses that exceeded RMS noise by a Z-score of least 3. RMS noise was calculated for each time point using the detrended traces recorded at the 3 lowest stimulus intensities (0.001%, 0.01%, and 0.1%), since none of the injured nerves showed apparent VEPs at these intensities. For each animal, the mean of these designated noise traces was normalized to 0 mV. We then measured the peak amplitudes of the responses to stimulation at 10% and 100%, and these were converted to Z-scores against the means noise at the corresponding time point. The presence of a VEP was defined by Z-score > 3. Chi-square analysis was used to compare the number of treated and untreated animals that showed VEPs in response to both the 10% and 100% stimuli.

Acknowledgements: We thank Drs. Farida Hellal and Frank Bradke for their assistance with the 3-DISCO clearing technique.

References

1. He Z. and Jin Y. (2016). Intrinsic Control of Axon Regeneration. Neuron 90, 437-51.
2. Filbin M.T. (2004). Myelin-associated inhibitors of axonal regeneration in the adult mammalian CNS. Nat. Rev. Neurosci. 4, 703-13.
3. Cajal R.Y. (1991). Cajal's Degeneration & Regeneration of the Nervous System. Oxford Press.
4. Galtrey C.M. and Fawcett, J.W. (2007). The role of chondroitin sulfate proteoglycans in regeneration and plasticity in the central nervous system. Brain Res. Rev. 54, 1-18.
5. Buchli A. D. and Schwab M.E. (2005). Inhibition of Nogo: a key strategy to increase regeneration, plasticity and functional recovery of the lesioned central nervous system. Ann. Med. 37, 556-67.
6. Park KK, Liu K, Hu Y, Smith PD, Wang C, Cai B, Xu B, Connolly L, Kramvis I, Sahin M and He Z. (2008). Promoting axon regeneration in the adult CNS by modulation of the PTEN/mTOR pathway. Science. 322,963-966.
7. Wu YY and Bradshaw RA. (1996). Induction of Neurite Outgrowth by Interleukin-6 Is Accompanied by Activation of Stat3 Signaling Pathway in a Variant PC12 Cell (E2) Line. JBC. 271, 13023-13032.
8. Quarta S, Baeumer BE, Scherbakov N, Andratsch M, Rose-John S, Dechant G, Bandtlow CE and Kress M. (2014). Peripheral Nerve Regeneration and NGF-Dependent Neurite

Outgrowth of Adult Sensory Nerurons Converge on STAT3 Phosphorylation Downstream of Neuropoietic Cytokine Receptor gp130. 34, 13222-13233.

9. Sun F, Park KK, Belin S, Wang D, Lu T, Chen G, Zhang K, Yeung C, Feng G, Yankner BA and He Z. (2011). Sustained axon regeneration induced by co-deletion of PTEN and SOCS3. Nature. 480,372-375.
10. Bei F, Lee HHC, Liu X, Gunner G, Jin H, Ma L, Wang C, Hou I, Hensch TK, Frank E, Sanes JR, Chen C, Fagiolini M and He Z. (2016). Restoration of Visual Function by Enhancing Conduction in Regenerated Axons. Cell. 164, 219-232.
11. Chandran V, Coppola G, Nawabi H, Omura T, Versano R, Huebner EA, Zhang A, Costigan M, Yekkirala A, Barrett L, Blesch A, Michaelevski I, Davis-Turak J, Gao F, Langfelder P, Horvath S, He Z, Benowitz L, Fainzilber M, Tuszynski M, Woolf CJ and Geschwind DH. (2016). A Systems-Level Analysis of the Peripheral Nerve Intrinsic Axonal Growth Program. Neuron. 89, 956-970.
12. Ram PT, Horvath CM, Iyengar R. (2000). Stat3-mediated transformation of NIH-3T3 cells by constitutively active Q2505L Galpho protein. Science 287, 142-4.
13. Jordan J.D., He J.C., Eungdamrong N.J., Gomes I., Ali W., Nguyeng T., Bivona T.G., Philips M.R., Devi L.A. and Iyengar R. (2005). Cannabinoid receptor-induced neurite outgrowth is mediated by Rap1 activation through G(alpha)o/i-triggered proteasomal degradation of Rap1GAPII. J. Biol. Chem. 280, 11413-21.
14. He J.C., Gomes I., Nguyeng T., Jayaram G., Ram P.T., Devi L.A. and Iyengar R. (2005). The G alpha(o/i)-coupled cannabinoid receptor-mediated neurite outgrowth involves Rap regulation of Src and Stat3. J. Biol. Chem. 280, 33426-34.

15. Bromberg K.D., Maayan A., Neves S.R. and Iyengar R. (2008). Design Logic of a cannabinoid receptor signaling network that triggers neurite outgrowth Science 320, 903-9.

16. Cao Z, Gao Y, Bryson JB, Hou J, Chaudhry N, Siddiq M, Martinez J, Spencer T, Carmel J, Hart RP and Filbin MT. (2006) The Cytokine Interleukin-6 Is Sufficient But Not Necessary to Mimic the Peripheral Conditiong Lesion Effect on Axonal Growth. J. Neurosci. 26,5565-5573.

17. Zorina Y., Iyengar R. and Bromberg K.D. (2010). Cannabinoid 1 receptor and interleukin-6 receptor together induce integration of protein kinase and transcription factor signaling to trigger neurite outgrowth. J. Biol. Chem. 285, 1358-70.

18. Yadaw A., Siddiq M., Rabinovich V., Iyengar R. and Hansen J. (2017). Dynamic balance between vesicle transport and microtubule growth enables neurite growth. bioRxiv doi: https://doi.org/10.1101/153569.

19. Hellal F., Hurtado A., Ruschel J., Flynn K.C., Laskowski C.J., Umlauf M., Kapitein L.C., Strikis D., Lemmon V., Bixby J., Hoogenraad C.C. and Bradke F. (2011). Microtubule stabilization reduces scarring and causes axon regeneration after spinal cord injury. Science 331, 928-931.

20. Mosnier L.O., Zlokovic B.V. and Griffin J.H. (2007). The cytoprotective protein C pathway. Blood. 109,3161-3172.

21. Wang Y., Zhao Z., Rege S.V., Wang M., Si G., Zhou Y., Wang S., Griffin J.H., Goldman S.A. and Zlokovic B.V. (2016). 3K3A-activated protein C stimulates postischemic neuronal repair by human neural stem cells in mice. Nature Med. 22. 1050-55.

22. Unpublished observations – Siddiq , Iyengar et al

23. Leon S., Yin Y., Nguyen J., Irwin N. and Benowitz L.I. (2000). Lens injury stimulates axon regeneration in the mature rat optic nerve. J. Neurosci. 20, 4615-4626.

24. Siddiq M.M., Hannila S.S., Carmel J.B., Bryson J.B., Hou J., Nikulina E., Willis M.R., Mellado W., Richman E.L., Hilaire M., Hart R.P. and Filbin M.T. (2015). Metallothionein-I/II Promotes Axonal Regeneration in the Central Nervous System. J. Biol. Chem. 290, 16343-16356.

25. Ertürk A., Mauch C.P., Hellal F., Förstner F., Keck T., Becker K., Jährling N., Steffens H., Richter M., Hübener M., et al. (2012). Three-dimensional imaging of the unsectioned adult spinal cord to assess axon regeneration and glial responses after injury. Nat. Med. 18, 166-171.

26. Mehta N.R., Lopez P.H., Vyas A.A. and Schnaar R.L. (2007). Gangliosides and Nogo receptors independently mediate myelin-associated glycoprotein inhibition of neurite outgrowth in different nerve cells. J. Biol. Chem. 282, 27875-86.

27. Fewou S.N., Plomp J.J. and Willison H.J. (2014). The pre-synaptic motor nerve terminal as a site for antibody-mediated neurotoxicity in autoimmune neuropathies and synaptopathies.

28. Sengottuvel V., Leibinger M., Pfreimer M. and Fischer D. (2011). Taxol facilitates axon regeneration in the mature CNS. J. Neurosci. 16, 2688-99.

29. Renier N., Wu Z., Simon D.J., Yang J., Ariel P. and Tessier-Lavigne M. (2014). iDISCO: A Simple, Rapid Method to Immunolabel Large Tissue Samples for Volume Imaging. Cell 159, 896-910.

30. Lu P., Wang Y., Graham L., McHale K., Gao M., Wu D., Brock J., Blesch A., Rosenzweig E.S., Havton L.A., Zheng B., Conner J.M., Marsala M. and Tuszynski M.H.

(2012). Long-Distance Growth and Connectivity of Neural Stem Cells After Severe Spinal Cord Injury. Cell 150, 1264-1273.

31. Fiorentini A., Maffei L., Pirchio M., Spinelli D. and Porciatti V. (1981) The ERG in response to alternating gratings in patients with diseases of the peripheral visual pathway. Invest. Opthalmol. Vis. Sci. 21, 490-3.
32. Husain S., Abdul Y. and Crosson C.E. (2012). Preservation of Retinal Ganglion Cell Function by Morphine in a Chronic Ocular-Hypertensive Rat Model. Invest. Opthalmol. Vis. Sci. 53, 4289-98.
33. Tang X., Tzekov R. and Passaglia C.L. (2016). Retinal cross talk in the mammalian visual system. J. Neurophysiol. 115, 3018-29.
34. Mukhopadhyay G., Doherty P., Walsh F.S., Crocker P.R. and Filbin M.T. (1994). A novel role for myelin-associated glycoprotein as an inhibitor of axonal regeneration. Neuron. 13, 757-67.

1-I

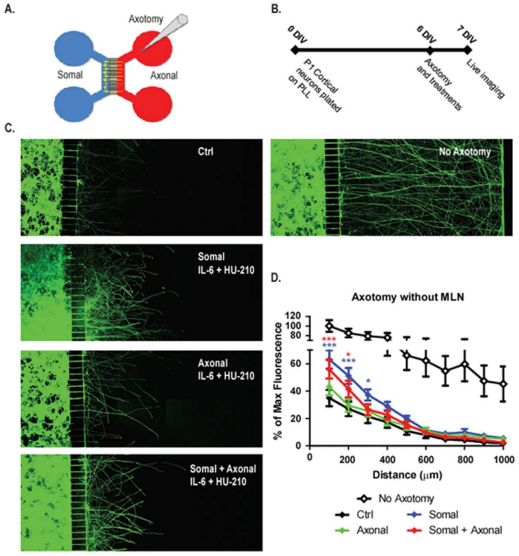

1-II

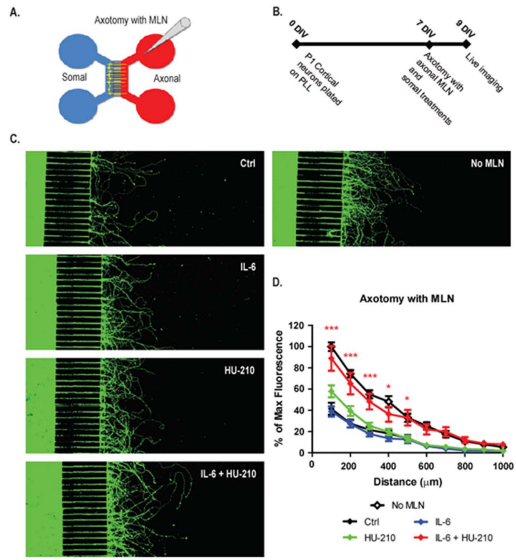

1-III

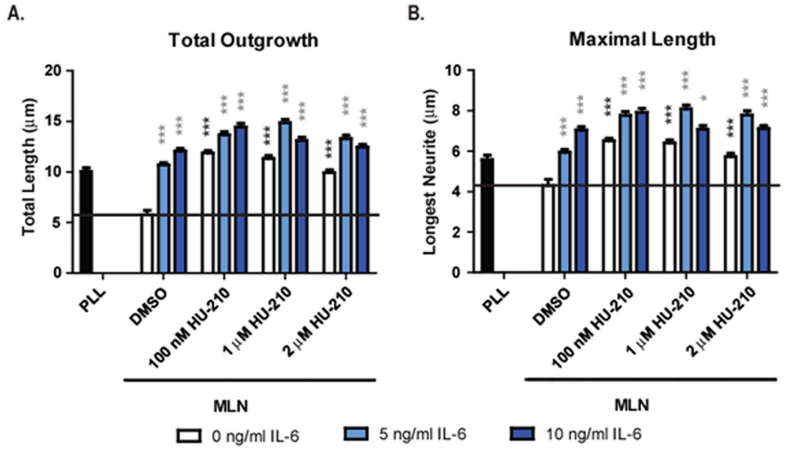

C.

Total Outgrowth	0 ng/ml IL-6	5 ng/ml IL-6	10 ng/ml IL-6
DMSO	0.00 ± 0.43	4.90 ± 0.25	6.27 ± 0.28
100 nM HU-210	6.07 ± 0.27	7.88 ± 0.31	8.67 ± 0.34
1 μM HU-210	5.54 ± 0.30	9.07 ± 0.35	7.31 ± 0.32
2 μM HU-210	4.14 ± 0.27	7.52 ± 0.33	6.66 ± 0.28

D.

Maximal Length	0 ng/ml IL-6	5 ng/ml IL-6	10 ng/ml IL-6
DMSO	0.00 ± 0.30	1.66 ± 0.12	2.75 ± 0.17
100 nM HU-210	2.22 ± 0.14	3.49 ± 0.18	3.63 ± 0.18
1 μM HU-210	2.10 ± 0.16	3.79 ± 0.19	2.80 ± 0.17
2 μM HU-210	1.44 ± 0.15	3.49 ± 0.20	2.82 ± 0.16

1-IV

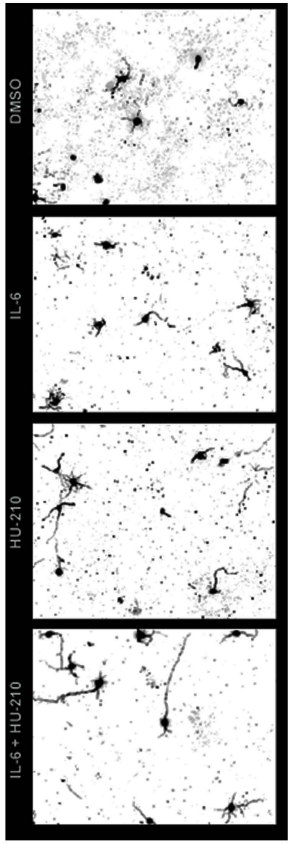

1-V

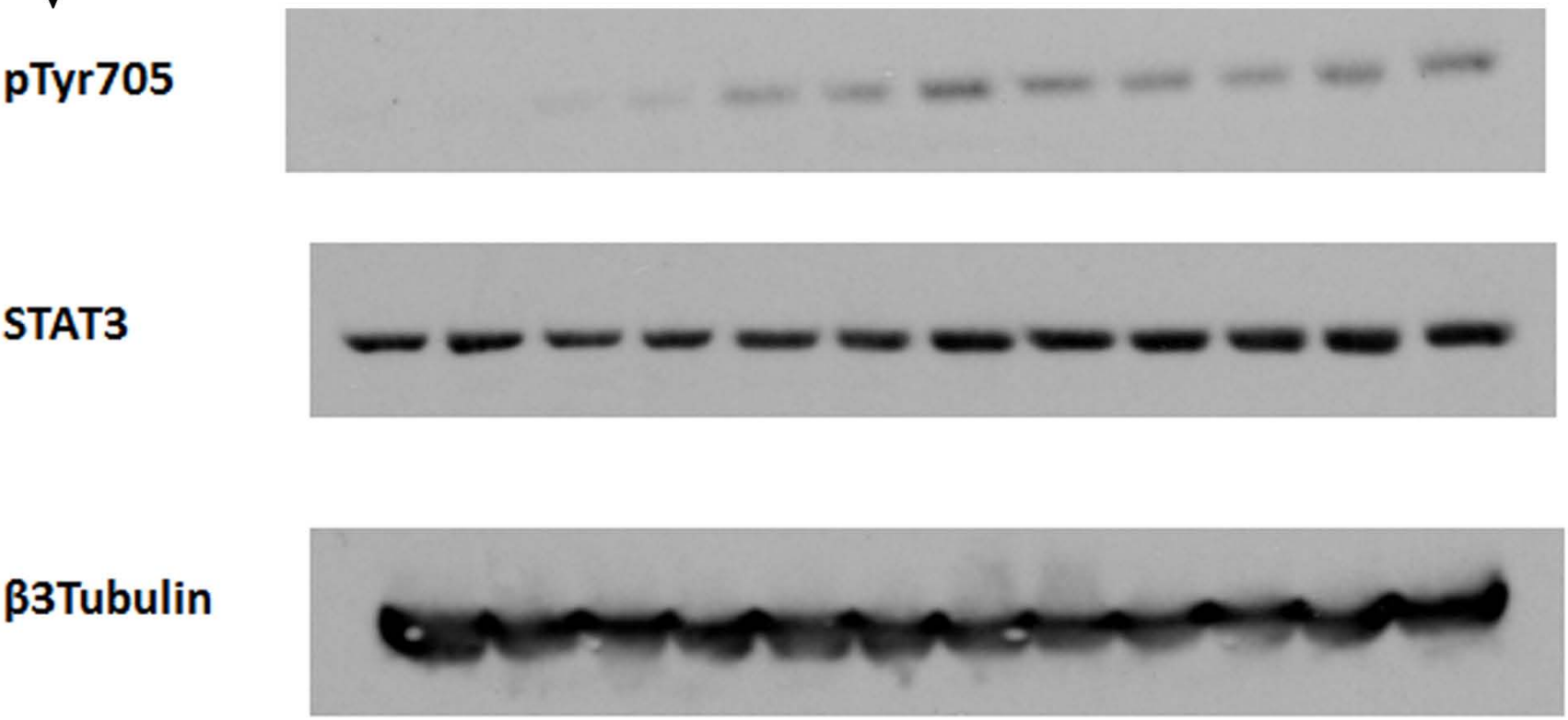

PBS	+	+	-	-	-	-	-	-	-	-	-	-
DMSO	-	-	+	+	-	-	-	-	-	-	-	-
IL-6 [ng/mL]	-	-	-	-	5	5	5	5	10	10	10	10
HU-210 [nm]	-	-	-	-	100	100	200	200	100	100	200	200

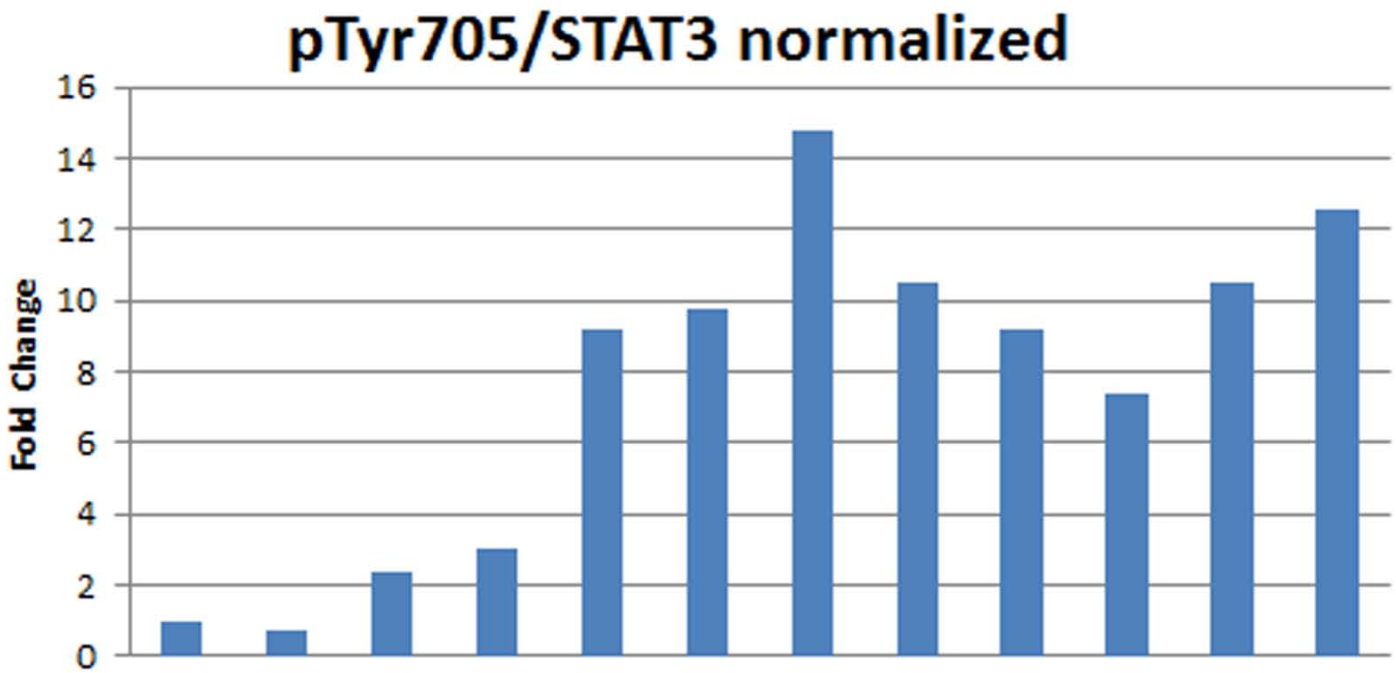

Figure 1-I. Somal application of IL-6 and HU-210 results in enhanced axonal regeneration after axotomy. Cortical neurons were plated in the somal compartment (blue) of microfluidic chambers, schematically represented in (A), and allowed to grow axons across the microgrooves into the axonal compartment (red). The gray cone depicts a pipet used to perform axotomy by aspirating medium from the axonal compartment. (B) For axotomy experiments, neurons were cultured in chambers on PLL for 6-7 days, switched to starving medium (NBS) for 1-2 h, and axotomy was performed by aspirating all medium from the axonal compartments 2-4 times. 5 ng/ml IL-6 and 100 nM HU-210 were added together to the somal, axonal, or both compartments after axotomy. Treatments were added to the indicated compartments in NBS immediately after axotomy, and neurons were imaged live after 24 h using Calcein AM. (C) Representative confocal images after axotomy and treatment. (D) Neurite outgrowth was quantified by measuring the total fluorescence at multiple cross-sections of the image. The zero point on the x-axis represents the right edge of microgrooves. All data points were normalized to the first point of "No Axotomy" at 100 µm from the microgrooves as 100 percent. Statistical differences were calculated from two independent experiments using two-way ANOVA. Asterisks show significance compared to Ctrl treatment at a given distance; *, $p < 0.05$; ***, $p < 0.001$.

Figure 1-II. Somal treatment with IL-6 and HU-210 promotes axonal regeneration on myelin. (A) Schematic representation of the microfluidic chamber. (B) Neurons were cultured in chambers on PLL for 7 days, switched to NBS for 1-2 h, and axotomy was performed. The axonal compartment was then filled with 20 µg/ml solution of myelin (MLN) in NBS. IL-6/HU-210 treatments were applied to the somal compartment of each respective chamber. The neurons were imaged live after 48 h using Calcein AM. (C) Representative confocal images of neurons following axotomy and treatment. (D) Neurite outgrowth was quantified by measuring the total fluorescence at multiple cross-sections of the image. The zero point on the x-axis represents the right edge of microgrooves. All data points were normalized to the first point of "No MLN" as 100 percent. Statistical differences were calculated from four independent experiments using two-way ANOVA. Asterisks show significance compared to Ctrl treatment at a given distance; *, $p < 0.05$; ***, $p < 0.001$.

Figure 1-III&IV. Stimulation of cortical neurons with IL-6 and HU-210 together promotes neurite outgrowth on myelin in a dose-dependent manner. P1 cortical neurons were plated on myelin–coated slides and treated with IL-6 and/or HU-210 over a range of concentrations. The neurons were fixed after 24 h and labeled for β-III-tubulin. Quantifications of neurite outgrowth were performed from 1500-2000 cells per condition. The bar graphs show mean ± S.E.M. of: (A) total length of neurites per cell; and (B) length of the longest neurite of each cell. Statistical differences were calculated using a one-way ANOVA followed by Bonferroni's multiple comparison test. Black asterisks show significance between the treatment and DMSO alone; gray asterisks show significance between each combinational treatment and the sole HU-210 treatment at the corresponding concentration; *, $p<0.05$; ***, $p<0.001$. (C-D) Tables show mean ± S.E.M. with value from DMSO treatment subtracted. Representative images of neurons

plated on myelin substrate treated from top to bottom, with either DMSO, IL-6, HU-210 alone, or IL-6 plus HU-210 labeled with β-III-tubulin.

Figure 1-V. Combination of IL-6 and HU-210 activates STAT-3. Cortical neurons in non-supplemented neurobasal media were treated with IL-6 and HU-210 or DMSO as control for 2 h. The cells were lysed and subjected to immunoblot analysis for phospho-STAT3 (p-Tyr705), total STAT3, and βIII-tubulin. We normalized the samples for phospho-STAT3 to total STAT3 and graphed the fold changes.

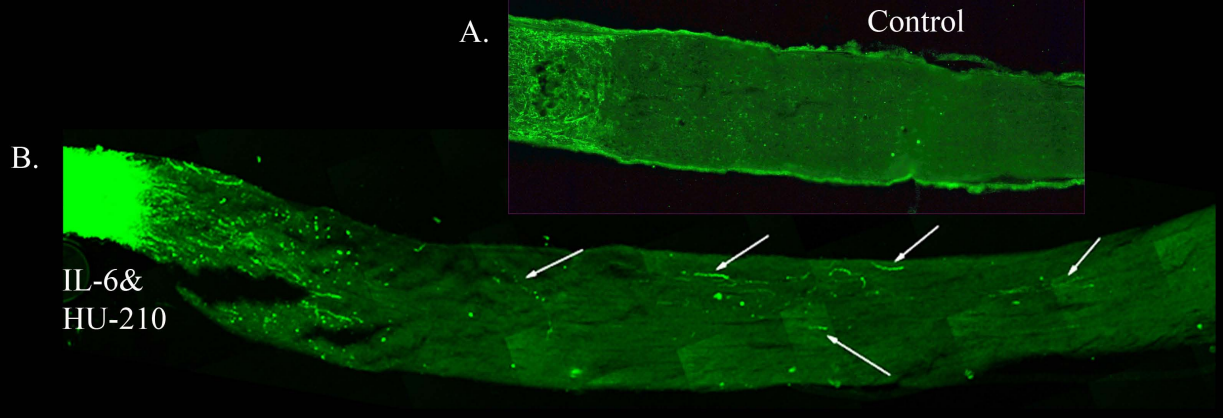

3-DISCO Clearing and Full nerve imaging of CTB-labeled axons

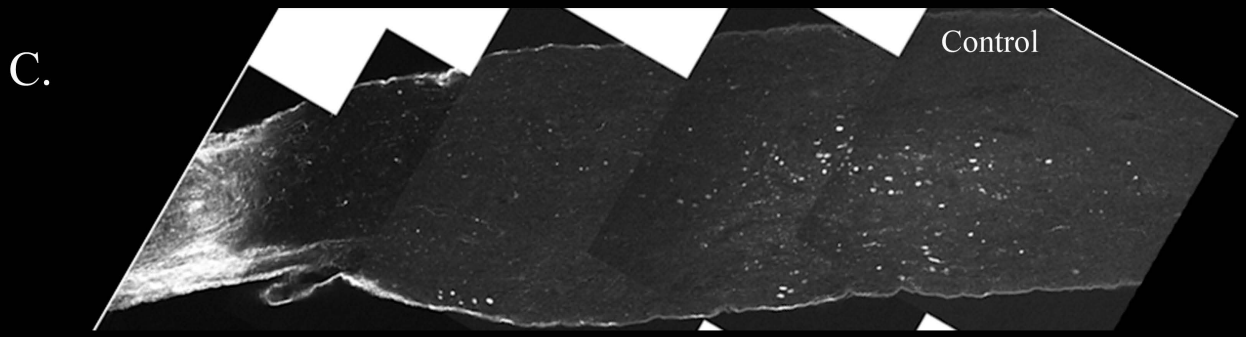

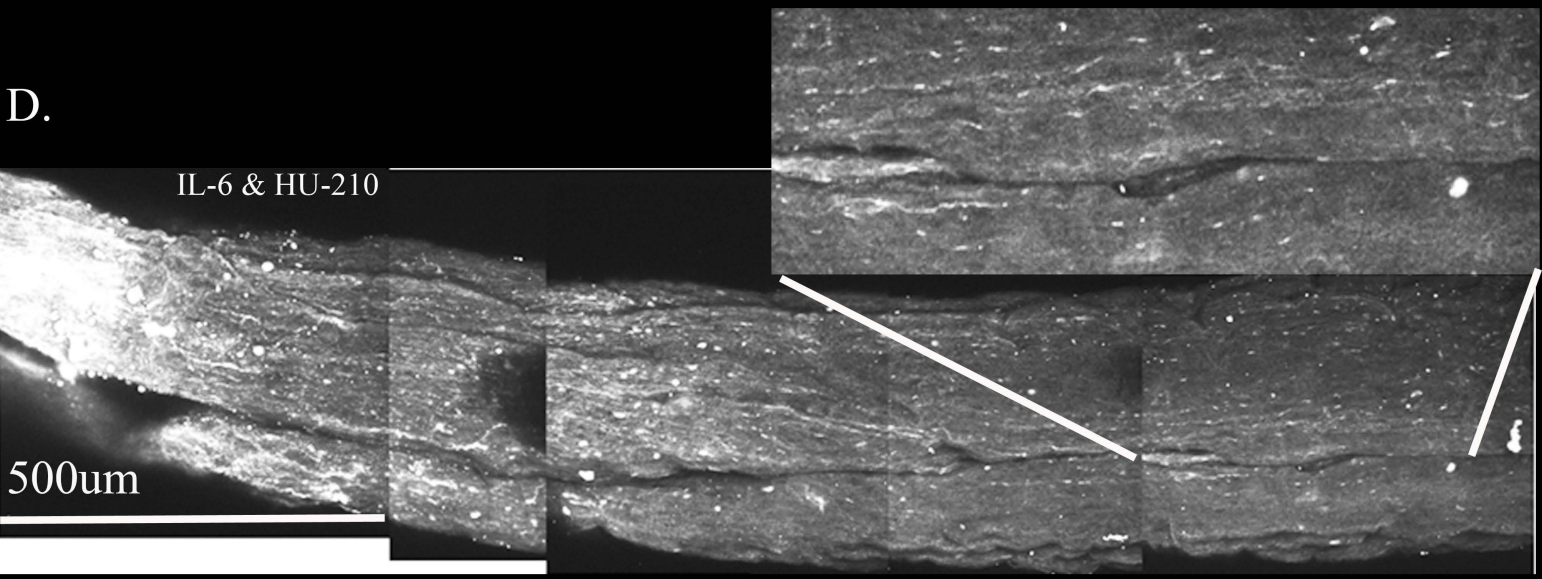

Figure 2. Combination of IL-6 and HU-210 injected intravitreally promotes axonal regeneration in the crushed rat optic nerve (ONC) model. Fischer adult rats had unilateral ONC performed followed by intravitreal injections of either 0.5% DMSO (A) for vehicle control or the combination of IL-6 and HU-210 (B). After 2 weeks the nerves were removed, sectioned and immunolabeled with GAP-43. Controls had clear crush sites but no GAP-43 labeled axons crossing the crush site, while IL-6 and HU-210 had regenerating axons nearly 3 mm away. CTB-labeled regenerating axons within the whole nerve were detected after applying the 3-DISCO clearing technique. Control animals (C) had clear crush sites with few fibers crossing. However, with IL-6 and HU-210 treatment we could detect CTB-labeled axons within the entire nerve bundle. In the box above panel D is a magnified region demarcated by the white bars, showing the extent of regenerating axons over 2 mm away from the crush site.

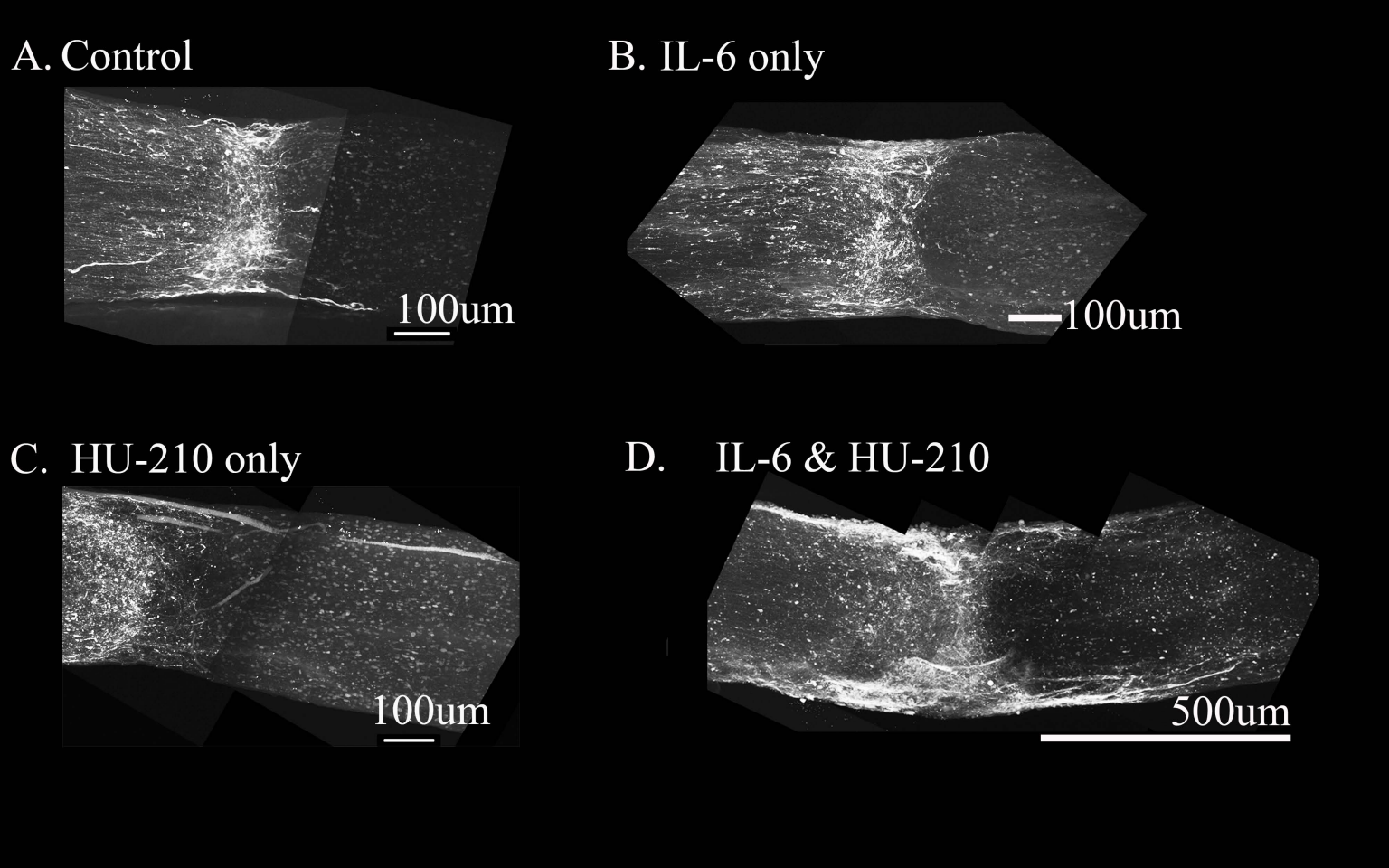
A. Control
100um
B. IL-6 only
100um
C. HU-210 only
100um
D. IL-6 & HU-210
500um

Figure 3. ONC axonal regeneration in response to the drugs tested in Long Evans Rats.

Using the rat ONC model and retrogradely labeling regenerating axons with Cholera Toxin B (CTB) by intravitreal injections into the retina 3 days prior to sacrificing and then chemical clearing using the 3-DISCO technique, we were visualizing the whole nerve and not just sections using a Multiphoton microscope. Control (A) not treated animals, have few labeled axons crossing a short distance (less than 0.2mm from the crush site), this was consistent for IL-6 (B) and HU-210 (C) tested individually as well, where no significant axonal regeneration was detected past the crush site. Combining intravitreal injections of IL-6 and HU-210 also promoted limited growth (D).

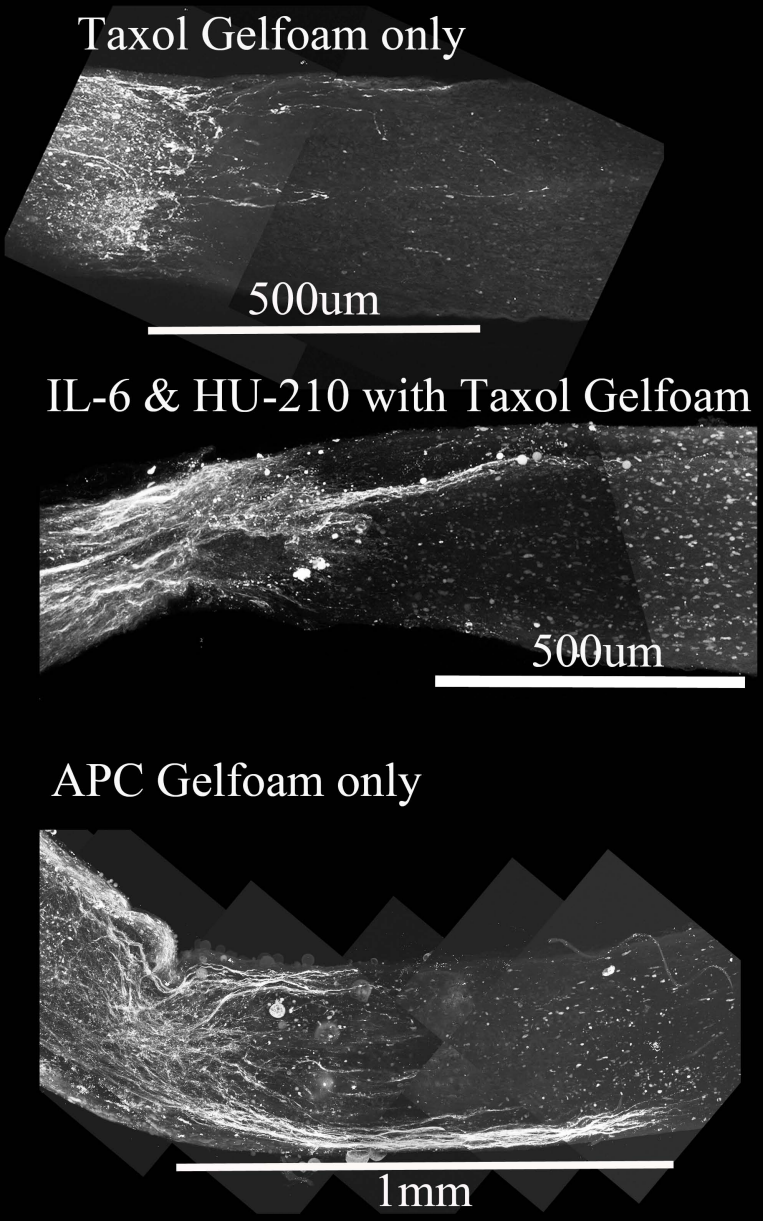
Taxol Gelfoam only
500um
IL-6 & HU-210 with Taxol Gelfoam
500um
APC Gelfoam only
1mm

Figure 4. Predicted Drugs applied in Gelfoam over the injury site promoted axonal regeneration.

Taxol applied in gelfoam alone had promoted limited axonal regeneration (A). Adding Taxol gelfoam with IL-6 and HU-210 injections resulted in more robust growth, but still less than 1mm from the crush site (B). APC gelfoam alone also promoted modest axonal regeneration from the crush site (C).

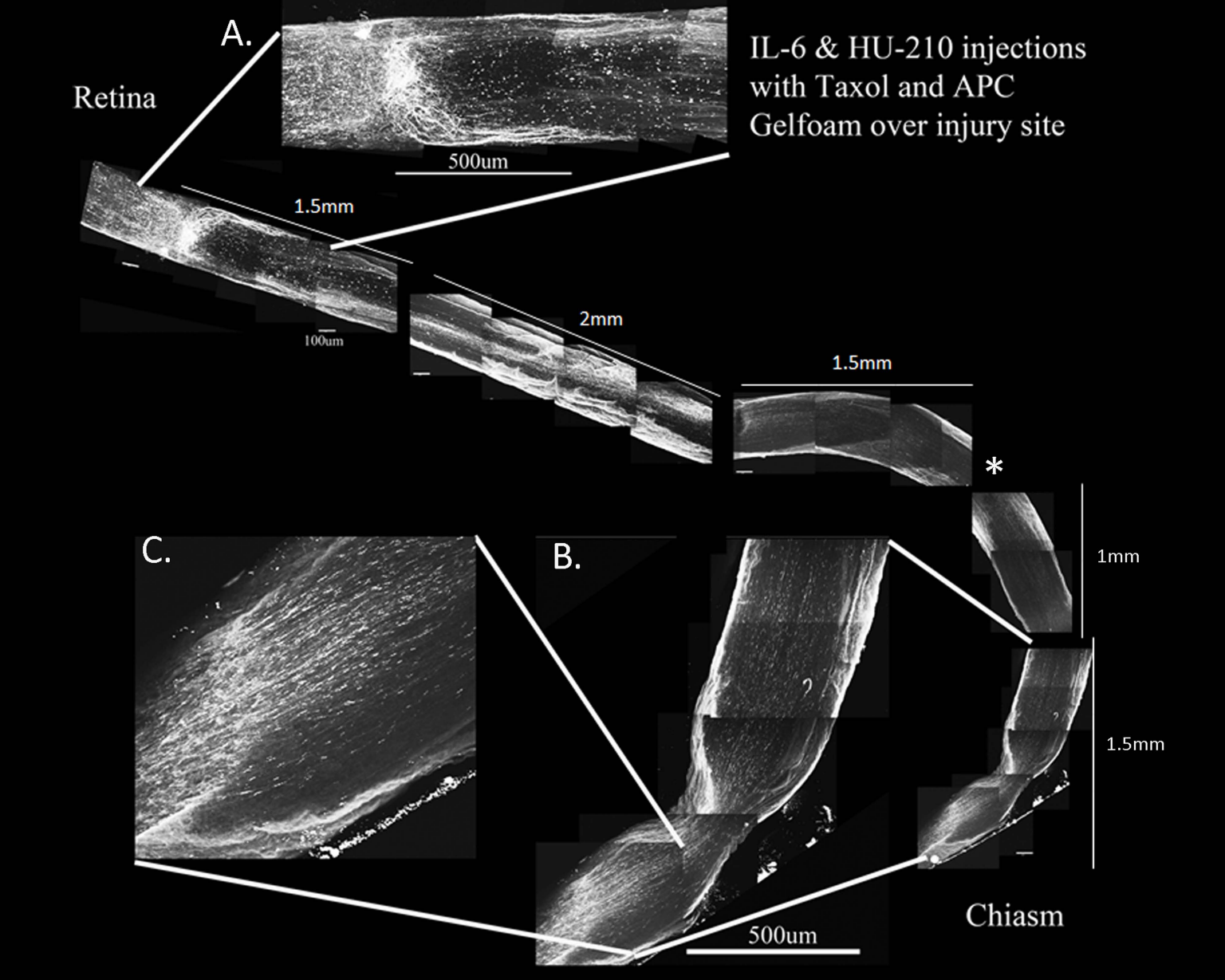
A.
Retina
500um
IL-6 & HU-210 injections
with Taxol and APC
Gelfoam over injury site
1.5mm
100um
2mm
1.5mm
*
C.
B.
1mm
1.5mm
500um
Chiasm

Figure 5. four-Drug combination in the rat ONC model promotes axonal regeneration to the chiasm. With four-Drug treatment we see abundant a synergistic effect where our four-drugs promoted CTB labeled axons that not only cross the crush site (A) but growing long distances, in this case all the way to the chiasm (B) which is nearly 8 mm away from the crush site (see arrows for enhanced panel of the chiasm in C). It is important to note that CTB-labeled axons closer to the retina (B1-2) appear more continuous, and the further the axons grow away from the retina to the chiasm, the more the they appear to have more punctate as seen in panels B and C.

Pattern Electroretinograms

A.

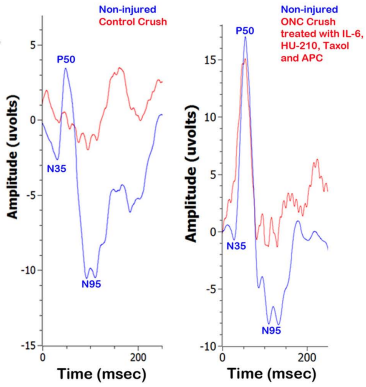

Voltage Evoked Potential (VEP)

B.

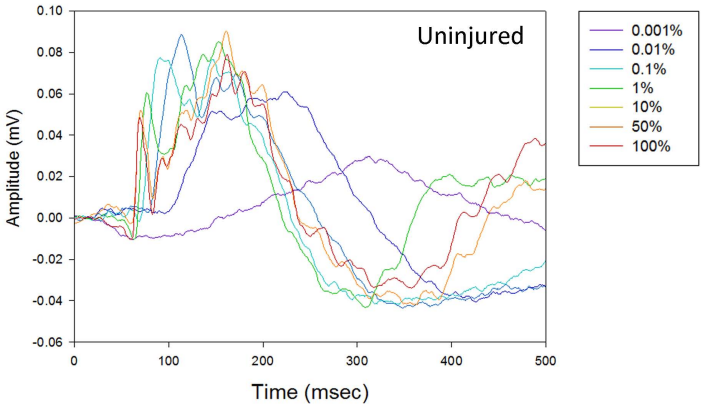

C.

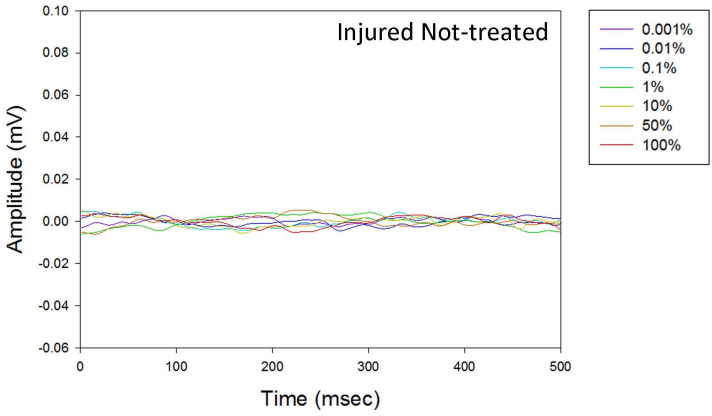

D.

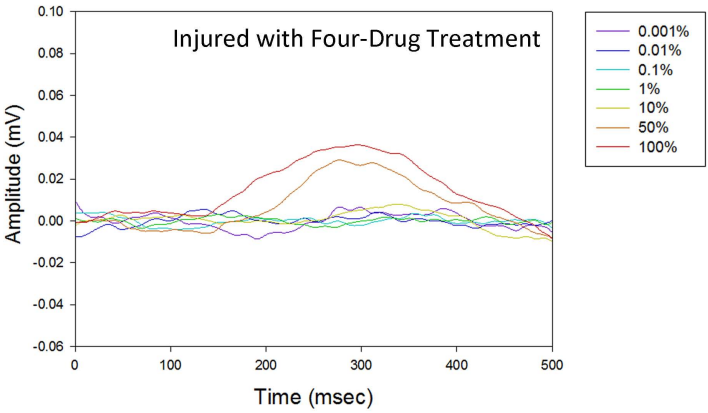

Figure 6. The four-drug combination enhances pattern electroretinograms and VEP responses compared to injured optic nerve treated with vehicle only. (A) We performed pattern electroretinograms (pERG) using the UTAS system (LKC Technologies). Two weeks after optic nerve crushes anesthetized animals had contact lens electrodes to record ERGs in response to pattern stimuli, we recorded from both the non-injured (blue) and injured (red) with (right panel) or without (left panel) the four-drug combination treatment. In representative recordings of control animals with vehicle only (left panel) had aberrant pERGs compared to their non-injured eye, while animals with the four-drug combination had pERGs in their injured eye (right panel) approaching baseline levels of their non-injured eye. These are individual raw recordings and not normalized. We performed flash electroretinograms (fERG, see Supplementary Figure 4) which is a strong response to the natural stimuli of light in a graded series of intensities (0.001 to 100% max flash intensity). (B-D) We simultaneously recorded visual evoked potentials (VEP bottom) in the brain. Flashes were delivered under dark adapted conditions. Uninjured nerve recordings had graded VEP response to increasing intensity of light. The VEP was slow for the dimmest flash, peaking around 300ms, and had fast onset with multiple wave components for the brightest flashes. Injured eyes with no treatment (Fig. 6C) have no detectable VEP activity. The VEP in several treated animals (Fig. 6D) exhibited a slow waveform in the response to the highest intensities of light (50 and 100%), suggesting that some axons regenerated all the way to the brain.

Table 1: Summary of Optic Nerve Regeneration in Long Evans Rats.

Treatment	Number of Animals tested	Regenerating axons not detected past crush site	Regenerating axons at least 3 mm from crush site	Regenerating axons to the chiasm (nearly 8 mm from crush site)
No treatment	11	11	0	0
4-Drug Combination	19	11	3	5